

Thermal expansion and theoretical density of 2,2',4,4',6,6'-hexanitrostilbene

Xiaoyan Shu · Yong Tian · Gongbao Song ·
Haobin Zhang · Bin Kang · Chaoyang Zhang ·
Yu Liu · Xiaofeng Liu · Jie Sun

Received: 26 September 2010/Accepted: 20 November 2010/Published online: 9 December 2010
© Springer Science+Business Media, LLC 2010

Abstract The linear coefficient of thermal expansion (CTE) and the theoretical density are important for energetic materials. To obtain the CTE and theoretical density of 2,2',4,4',6,6'-hexanitrostilbene (HNS), X-ray powder diffraction (XRD) together with Rietveld refinement was employed to estimate the dimension and density change at a crystal lattice level, in the range of temperature 30–240 °C. The CTE of *a*-, *b*-, *c*-axis and volume were obtained as $7.6719 \times 10^{-5}/\text{°C}$, $6.8044 \times 10^{-5}/\text{°C}$, $1.1192 \times 10^{-5}/\text{°C}$ and $16.725 \times 10^{-5}/\text{°C}$, respectively. Also, the possible reasons for the expansion property of HNS have been discussed by comparing its structure with 1,3,5-triamino-2,4,6-trinitrobenzene (TATB). Based on the refined lattice parameters, the theoretical densities of HNS at various temperatures were obtained. By extrapolation of linear fitting the theoretical density of HNS at 20 °C was gotten as 1.7453 g/cm³. Furthermore, a good thermal resilience of HNS has also been observed when the temperature returned from 240 to 30 °C.

Abbreviations

CTE	Coefficient of thermal expansion
HNS	2,2',4,4',6,6'-Hexanitrostilbene
XRD	X-ray powder diffraction
TATB	1,3,5-Triamino-2,4,6-trinitrobenzene

X. Shu · G. Song
School of Materials Science and Engineering, Southwest University of Science and Technology, Mianyang 621010, Sichuan, People's Republic of China

X. Shu · Y. Tian · H. Zhang · B. Kang · C. Zhang · Y. Liu · X. Liu · J. Sun (✉)
Institute of Chemical Materials, China Academy of Engineering Physics, Mianyang 621900, Sichuan, People's Republic of China
e-mail: zhuoshisun@sina.com

HEMs High energy materials

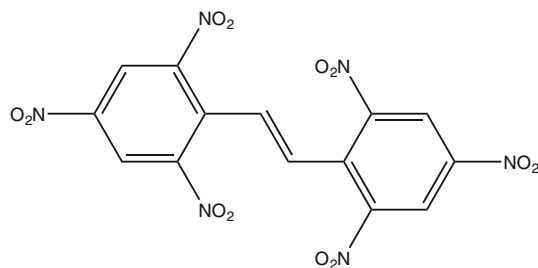
HPLC High-performance liquid chromatography

Introduction

Since HNS was synthesized by reacting a solution of tri-nitrotoluene (TNT) with sodium hypochlorite (NaOCl) for the first time in 1964 [1], some other methods for preparation of HNS have been reported [2–4]. One new job about that was just done by A. J. Bellamy, through his extended method an improvement over the conventional batch process was achieved, and the yield and selectivity was also significantly enhanced [5]. Figure 1 shows the molecular structure of HNS. It is a typical heat-resistant explosive, and due to its excellent thermal stability, it is widely used as energetic ingredients in thermally stable charges where it may encounter high temperatures [6], such as in supersonic missiles and in crude oil production.

Except for preparation, the experimental researches of HNS are mostly focused on the thermal decomposition behaviour of HNS [7, 8], while the ignition and combustion performance, propagation capability of detonation, potential energy surface, and formulation in booster explosive have also been researched at some extent. The theoretical researches about HNS are plentiful, including various thermodynamic properties, detonation properties, molecular structure, packing structure, electronic structures and energy and so on [9–15].

The linear CTE and theoretical density are important properties for most materials [16, 17], and they could influence the ultimate performance of high energy materials (HEMs) [18]. However, it is the fact that the properties of HNS with increasing temperature have seldom been considered in the past. To the best of our knowledge, no

**Fig. 1** The molecular structure of HNS

investigation about CTE of HNS crystal has been reported, and there is no report on the density changes versus temperature about HNS either. On the other hand, the vital information of its theoretical density is variously reported even in authoritative databases, just as shown in Table 1.

In this paper, X-ray powder diffraction was employed in the temperature range of 30–240 °C to get XRD patterns of HNS at various temperatures. Then based on the obtained patterns, Rietveld refinement was applied in Topas 3.0 program to get the lattice parameters of HNS, through which the vital information of crystal structure could be achieved. So the linear CTE and theoretical density would be obtained. Furthermore, the thermal resilience of HNS from 240 to 30 °C was also discussed in this study.

Experiment

The sample of HNS used for XRD measurement was offered by the Institute of Chemical Materials, China Academy of Engineering Physics. The mean particle size was about 20 µm, with the central 80% between 10 and 30 µm, and its purity is measured to be 99.5% by HPLC.

X-ray diffraction data were collected through a Bruker D8 Advance X-ray diffractometer by using Cu K α radiation without taking monochromator. A TTK 450 temperature chamber was used to precisely control the temperature during experiment. The X-ray tube operating conditions were set as 40 kV and 40 mA, while Vantec-1 detector was adopted during experiment. At every tested temperature point, the sample was scanned from 10° to 70° in 2 θ , with a step width of 0.02° and the counting time was set as 0.2 s per step.

A series of XRD detection were undertaken all through the temperature cycle, and the detailed scheme was just as follows. First raise the temperature from 30 to 240 °C, at the rate of 0.1 °C/s, and the scanning data was collected at every increased 30 °C. After that, the temperature was drawn back at the same rate, from 240 to 30 °C. Also, the XRD measurement was carried out during cooling-down to study the resilience of HNS.

To estimate the dimensional changes influenced by temperature variation, the obtained diffraction patterns were refined using the programme Topas 3.0 with the method of Rietveld analysis. The observed line profile fitting will be performed using fundamental parameters approach (FPA). The instrument parameters were mentioned in previous work [18].

The crystal cell parameters of HNS used as initial values for Rietveld refinement are shown in Table 1 (PDF: 044-1629), and P 21/c was input as space group. It is needed to point out here that the parameters used for Rietveld refinement must be roughly accurate to ensure the convergence of refinement.

Results and discussion

Thermal expansion of HNS

Within the temperature cycle from 30 to 240 °C and then back to 30 °C, the diffraction patterns were collected at every changed 30 °C. During heating, no other changes could be observed except a decrease of 2 θ , and the excursion of the crystalline plane (4 1 0) amounted to 0.3657° at 240 °C. The XRD patterns of HNS at 30 °C, both for initial and final sample, and that at 240 °C are displayed in Fig. 2. It could be indicated from these patterns that no phase transformation but expansion of the lattice has taken place within the temperature range.

Based on the X-ray powder diffraction patterns, Rietveld fitting method together with Topas 3 software was employed to get the refined lattice parameters of HNS corresponding to certain temperature points. The lattice parameters a , b , c , β , the volume, the density and R_{wp} (weighted profile R factor) are summarized in Table 2.

To make it clear, the refined lattice parameters have been plotted as a function of temperature, and the values of

Table 1 Lattice parameters of HNS in ICDD databases

No.	a (Å)	b (Å)	c (Å)	α (°)	β (°)	γ (°)	V (Å 3)	ρ (g cm $^{-3}$)	T (K)	Remarks
1	22.326	5.5706	14.667	90.00	110.04	90.00	1713.68	1.745	–	PDF (044-1629)
2	22.083	5.554	14.634	90.00	108.45	90.00	1702.59	1.756	283–303	NBS Id (586879)
3	22.328	5.576	14.559	90.00	109.56	90.00	1708.01	1.751	–	PDF (042-1919)

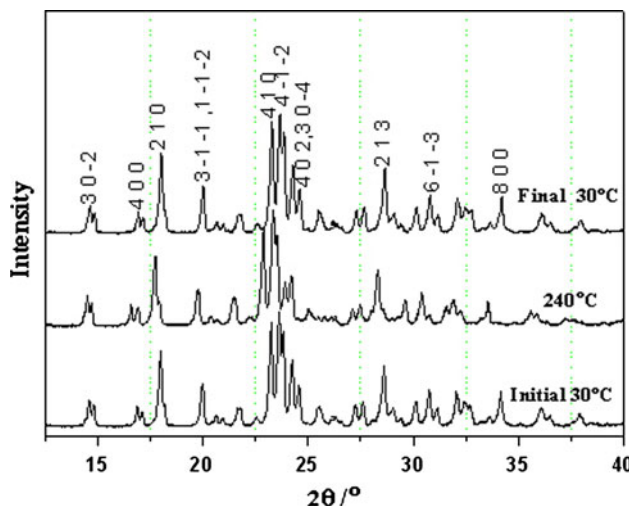


Fig. 2 XRD patterns of HNS at various temperatures

correlation coefficient in linear fitting (R^2) are given in Fig. 3 for each diagram.

In these diagrams, the square denotes the corresponding parameters obtained from the heating course, and the dot means the information getting from cooling; α here means coefficient of parameter change towards temperature, which comes from the linear fitting during heating.

It could be observed that the discussed parameters have perfectly reverted to the previous state during cooling. By comparing the initial and final XRD patterns of HNS at 30 °C (in Fig. 2), the same result could also be achieved. So, the thermal resilience of HNS has been revealed here, and this is meaningful for the actual performance of HNS, which may suffer thermal stimulation repeatedly.

Figure 3 shows obvious linear $P-T$ correlations, and the correlation coefficients (R^2) distribute from 0.9862 to 0.9998. However, it could be noted that the linearity and thermal resilience of c -axis is not as good as that of others. This may be caused by the slighter expansion along c -axis within the same temperature range, as the relative expansion value at a -axis and b -axis were approximately seven and six times of that at the c -axis, respectively. It implies that a smaller range of Y -axis is depicted within the same scope of X -axis for c -axis, the distinction seems to be more obvious relatively. This situation is similar with that in TATB at a -, b -axis [19].

It is easy to get known of the linear CTE of a -, b -, c -axis as about $7.6719 \times 10^{-5}/^\circ\text{C}$, $6.8044 \times 10^{-5}/^\circ\text{C}$ and $1.1192 \times 10^{-5}/^\circ\text{C}$, and the CTE for volume is about $1.6725 \times 10^{-4}/^\circ\text{C}$. The beta shows a little decrease while the volume increases about 3.47% from 30 to 240 °C. Evidently, a -axis shows the similar thermal expansion with b -axis, while the thermal expansion of c -axis is only about 1/7 of that along a -axis. So, an anisotropic thermal expansion of HNS is revealed here.

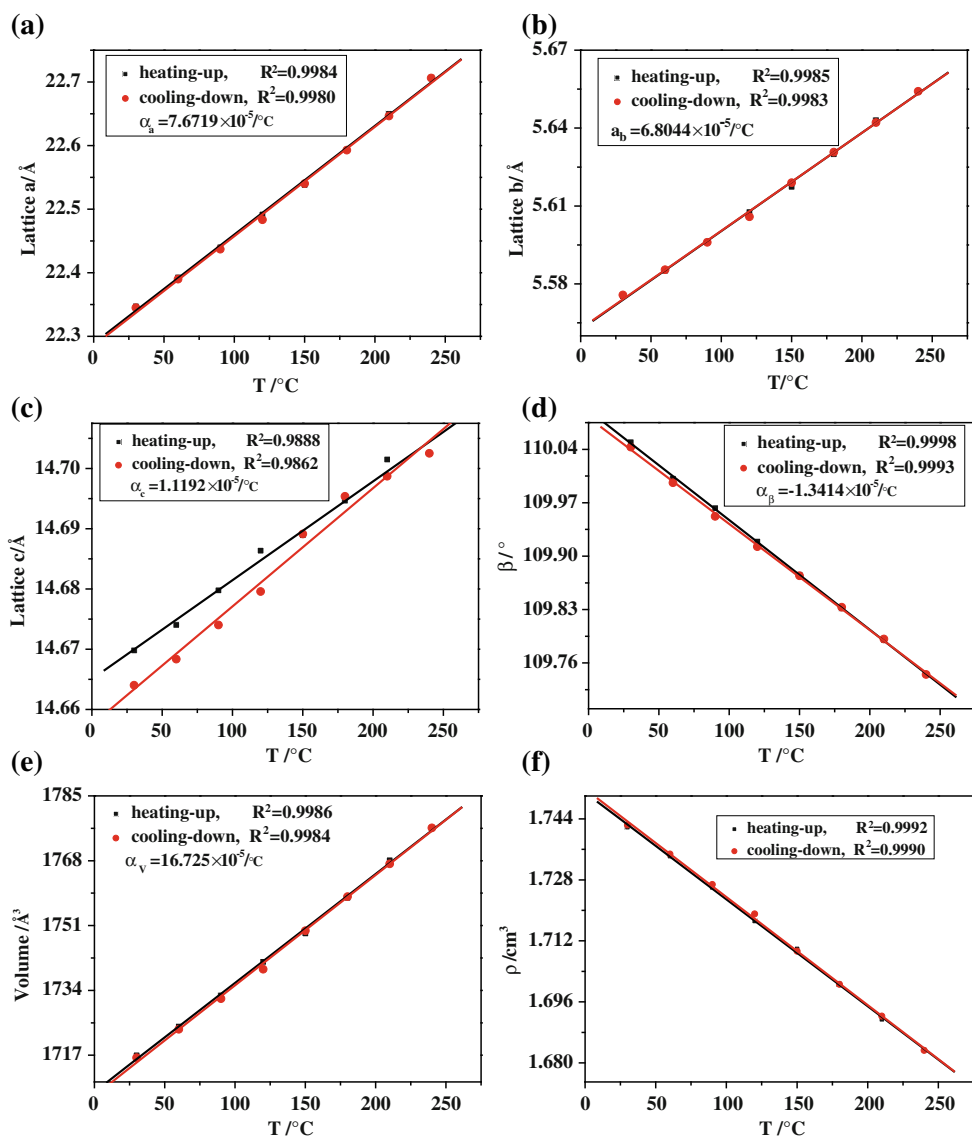
As another commonly used nitro compound, TATB exhibits anisotropic expansion also when subjected to thermal variation, which has been revealed in our lab research before [19]. However, the thermal expansion along c -axis in TATB molecule is completely another case when compared with that of HNS, it is about 20 times larger than that along a -axis and b -axis direction. The phenomena may root in the following two aspects. First the π -stacking interactions should be pointed out, just as shown in Fig. 4, there are T-shaped π -stacking interactions in HNS (a), while there are big and reciprocally parallel π systems exist in TATB (b) [20]. And the different

Table 2 Refined lattice parameters of HNS at elevated temperatures

T (°C)	a (Å)	b (Å)	c (Å)	β (°)	Volume (Å 3)	Density (g cm $^{-3}$)	Rwp ^a (%)
30	22.3472	5.5753	14.6698	110.05	1716.98	1.7418	8.44
60	22.3927	5.5851	14.6740	110.00	1724.51	1.7342	8.21
90	22.4400	5.5961	14.6798	109.96	1732.67	1.7260	8.33
120	22.4915	5.6076	14.6864	109.92	1741.49	1.7172	8.68
150	22.5382	5.6174	14.6889	109.88	1748.94	1.7099	9.07
180	22.5931	5.6300	14.6947	109.83	1758.29	1.7008	9.55
210	22.6501	5.6431	14.7015	109.79	1768.10	1.6914	10.29
240	22.7062	5.6542	14.7025	109.74	1776.61	1.6833	11.08
210	22.6465	5.6422	14.6987	109.79	1767.19	1.6923	10.23
180	22.5928	5.6308	14.6954	109.83	1758.58	1.7006	9.68
150	22.5403	5.6190	14.6891	109.87	1749.63	1.7093	9.03
120	22.4833	5.6059	14.6796	109.91	1739.58	1.7191	8.80
90	22.4370	5.5960	14.6740	109.95	1731.85	1.7268	8.39
60	22.3901	5.5855	14.6684	110.00	1723.83	1.7348	8.34
30	22.3450	5.5757	14.6640	110.043	1716.34	1.7424	8.21

^a Rwp is used as a factor to comment on the refinement results, and it is common to deem the results as reliable while Rwp < 15%

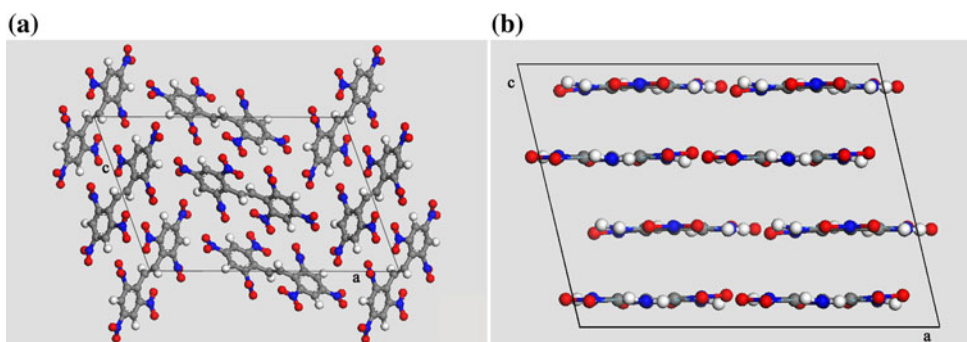
Fig. 3 Lattice parameters of a -, b -, c -axis, volume and measured density of HNS during heating-up and cooling-down as depicted in (a–f)



π -stacking way may contribute to the varied distribution of atoms along c -axis. As shown in Fig. 4, the even distributed atoms along three directions in HNS crystal make little discrepancy in interactions among atoms during expansion or shrink, while the less denseness of atoms along c -axis in TATB results in the weaker resistance

comes from adjacent atoms, and this makes TATB tend to expand or shrink along c -axis towards changed temperature. Furthermore, the special crystalline anisotropy in TATB might be taken as another reason. The strong network comprised of hydrogen bond within a -, b -plane makes TATB more stable along a , b -axis, while the poor

Fig. 4 Supercell diagrams of **a** HNS and **b** TATB



interaction among molecules makes the contact relative loose along *c*-axis direction, and that maybe the reason why α_c of HNS is much smaller than TATB, whereas, there is scarcely any effect caused by hydrogen bond in HNS crystal, because all of hydrogen atoms are connected firmly with carbon atoms.

Furthermore, the relation of density versus temperature could be obtained through linear fitting, and it could be expressed by the following equation:

$$\rho = 1.7509 - 2.8032 \times 10^{-4} \times T \quad (1)$$

That means the density of HNS decreased versus growing temperature with the coefficient of 2.8032×10^{-4} (given in Fig. 3). Equation 1 also indicates that a shift of 0.001 g/cm^3 in density could be induced by about every changed 4°C .

Through Eq. 1 it is convenient to get the theoretical density of HNS at certain temperatures. And the theoretical density at 20°C has been obtained as 1.7453 g/cm^3 . This result is in close match with that given by PDF: 00-044-1629, which means a preferable choice for users has been confirmed, while it also means that the adopted method in this paper is reliable for theoretical density measurement of explosives.

Conclusion

By means of X-ray powder diffraction and Rietveld refinement, an anisotropic thermal expansion of HNS has been revealed, while the coefficient of thermal expansion of HNS crystal has been obtained. Furthermore, through the refined crystalline parameters, the calculating method about the theoretical density of HNS at various temperatures has also been given out. The theoretical density for HNS at 20°C is in close match with the reported value,

which displays the convenience and reliability of this method in density determination. Meanwhile, an obvious thermal resilience of HNS crystal has also been revealed.

Acknowledgements This work is supported by the National Science Foundation (No. 10979037); the National Defence Item 973 (No. 61383); the Science Foundation of China Academy of Engineering Physics (No. 2009A0203010), China.

References

- Shipp KG (1964) Org Chem 29:2620
- Sollott GP (1982) Org Chem 47:2471
- Wang JY, Huang H, Xu WZ et al (2009) J Hazard Mater 162:842
- Teipel U, Leisinger K, Mikonsaari I (2004) Int J Miner Process 74:183
- Bellamy AJ (2010) Org Process Res Dev 14:632
- Nair UR, Gore GM et al (2006) J Hazard Mater 143:500
- Dominik C, Rudolf KP (2007) Propell Explos Pyrot 32(4):322
- Rieckmann Th, Volker S, Lichtblau L, Schirra R (2001) Chem Eng Sci 56:1327
- Muthurajan H, Sivabalan R et al (2006) J Hazard Mater A 133:30
- Muthurajan H, Sivabalan R et al (2006) J Hazard Mater A 136:475
- Victorov SB, Gubin SA (2006) ShockWaves 15(2):113
- Wang GX, Shi CH, Gong XD et al (2009) J Hazard Mater 169:813
- Mehlhorn A, Fabian J, Gabriel W et al (1995) J Mol Struct 339:215
- Zhu WH, Shi CH, Xiao HM (2009) J Mol Struct 910:148
- Wasilewskit J, Staemmler V (1986) Inorg Chem 25:4221
- Stefano G, Francesco M (2010) J Mater Sci 45:824. doi: [10.1007/s10853-009-4006-6](https://doi.org/10.1007/s10853-009-4006-6)
- Mallawany R, Abdel-Kader A et al (2010) J Mater Sci 45:871. doi: [10.1007/s10853-009-4015-5](https://doi.org/10.1007/s10853-009-4015-5)
- Xue C, Sun J, Kang B et al (2010) Propell Explos Pyrot 35:333
- Sun J, Kang B, Xue C et al (2010) J Energ Mater 3:189
- Zhang CY, Wang XC, Huang H (2008) J Am Chem Soc 130:8359